Magnetization plateaus of spin-$\frac{1}{2}$ system on a 5/7 skewed ladder

Dayasindhu Dey,[1] Sambunath Das,[1] Manoranjan Kumar,[2,*] and S. Ramasesha[1,†]
[1]*Solid State and Structural Chemistry Unit, Indian Institute of Science, Bangalore 560012, India*
[2]*S. N. Bose National Centre for Basic Sciences, Block-JD, Sector-III, Salt Lake, Kolkata 700106, India*

(Received 22 January 2020; revised manuscript received 19 March 2020; accepted 14 April 2020; published 5 May 2020)

Magnetization plateaus are some of the most striking manifestations of frustration in low-dimensional spin systems. We present numerical studies of magnetization plateaus in the fascinating spin-1/2 skewed ladder system obtained by alternately fusing five- and seven-membered rings. This system exhibits three significant plateaus at $m = 1/4$, $1/2$, and $3/4$, consistent with the Oshikawa-Yamanaka-Affleck condition. Our numerical as well as perturbative analysis shows that the ground state can be approximated by three weakly coupled singlet dimers and two free spins, in the absence of a magnetic field. With increasing applied magnetic field, the dimers progressively become triplets with large energy gaps to excited states, giving rise to stable magnetization plateaus. Finite-temperature studies show that $m = 1/4$ and $1/2$ plateaus are robust and survive thermal fluctuations while the $m = 3/4$ plateau shrinks rapidly due to thermal noise. The cusps at the ends of a plateau follow the algebraic square-root dependence on B.

DOI: 10.1103/PhysRevB.101.195110

I. INTRODUCTION

The study of quantum phase transitions in frustrated low-dimensional magnets has been an active area of research in the past few decades. The simplest model of a frustrated magnet is the one-dimensional (1D) J_1-J_2 model, where each spin is interacting with its nearest and next nearest neighbors with exchange parameters of strength J_1 and J_2, respectively [1–21]. This system can be mapped onto a zigzag ladder if odd and even sites of the chain are arranged on the two legs of the ladder, as shown in Fig. 1(a). The frustration in these magnetic systems can give rise to many exotic phases in the ground state (gs), such as gapless spin liquid [2,5–7,9,10], dimers [1–11], and spiral phases [3,5,7,8,10,12] in the absence of an applied magnetic field B. These systems become a veritable zoo of phases in the presence of a finite magnetic field B [8,13–19]; for example, a system with exchange interactions J_1 (ferromagnetic) and J_2 (antiferromagnetic) shows multi-magnon condensation [14,15,20–22], a vector chiral phase [3,14,15,22], and magnetization plateaus [18,23,24]. In addition to a magnetization plateau phase, frustrated systems can also show kinks and jumps in magnetization [18].

There have been several recent attempts to gain a theoretical understanding of the magnetization process in quantum spin chains and ladders [18,23–33]. The magnetization plateau indicates the existence of energy gaps between two consecutive magnetic spin sectors in the thermodynamic limit, and one such example is the integer spin Heisenberg antiferromagnetic (HAF) chain [34–36]. The energy gap between the gs ($S = 0$) and the next magnetic excited state ($S = 1$) is finite for an integer spin chain with a periodic boundary condition, which is the well-known Haldane gap [34–36]. Therefore, there is an $M = 0$ plateau in the gs, and a finite field B of strength $\frac{E_g}{g\mu_B}$ (E_g is the Haldane gap, g is the gyromagnetic ratio, and μ_B is the Bohr magneton) is required to spin-polarize the system. In fact, the Heisenberg spin-1 chain with single ion anisotropy also shows a plateau at $m = M/M_{\max} = 1/2$, where M is the magnetization at the plateau and $M_{\max}$ is the saturation magnetization [37]. The 1D J_1-J_2 model with exchange interactions J_1 (ferromagnetic) and J_2 (antiferromagnetic) as well as both antiferromagnetic J_1 and J_2 shows plateaus at m values of 0 and $1/3$ for $|J_2/J_1| > 0.6$ [18,23,24]. The magnetization plateau at $m = 0$ has also been predicted for the ordinary two-legged ladder, which has finite spin gap in the gs [25,26]. In the 2D system, magnetization plateaus in a kagomé lattice are predicted to be at $m = 1/9$, $1/3$, $5/9$, and $7/9$ [38–43], whereas for a triangular lattice, the magnetization plateau appears at $m = 1/3$ [44].

Experimentally, the magnetization plateau at $m = 1/3$ is found in frustrated spin chains such as $Cu_3(CO_3)_2(OH)_2$ [45–47] and the spin-1/2 trimer compound $Cu_3(P_2O_6OH)_2$ [48]. Other compounds showing a $1/3$ plateau are $Ca_3Co_2O_6$ [49–51], $Sr_3Co_2O_6$ [52], Sr_3HoCrO_6 [53], $SrCo_6O_{11}$ [54], and CoV_2O_6 [55–57]. The frustrated ladder compound NH_4CuCl_3 [58] shows two plateaus at $m = 1/4$ and $3/4$.

Oshikawa, Yamanaka, and Affleck (OYA) [25] established the necessary condition for the occurrence of plateaus in a 1D spin-S system by generalizing the Lieb-Schultz-Mattis (LSM) theorem [36,59]. The OYA condition for observing a plateau at m is given by $Sp(1 - m) \in \mathbb{Z}$, where S is the spin of a site, p is the number of lattice sites per unit cell, and $\mathbb{Z}$ represents the set of positive integers. The condition is further generalized to n-leg ladder [26,60], which is given as $nSp(1 - m) \in \mathbb{Z}$. The Haldane chain is a special case of this condition in

*manoranjan.kumar@bose.res.in
†ramasesh@sscu.iisc.ernet.in

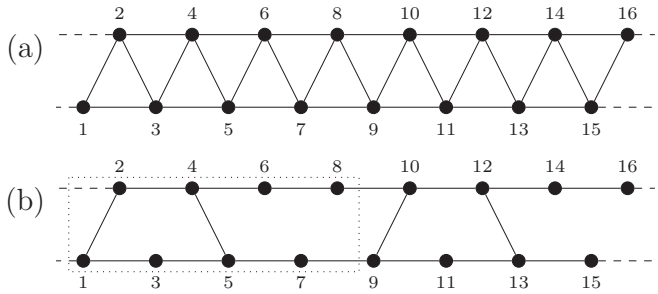

FIG. 1. (a) The regular zigzag chain and (b) the 5/7 skewed ladder lattice. A unit cell consisting of eight spins is shown in the box with dotted edges.

which $n = p = 1$, and for integer S a plateau could occur at $m = 0$.

In this paper we are interested in the skewed ladder system, which is a variant of a zigzag ladder with periodically missing rung bonds [61]. The 5/7 system, which corresponds to fused azulenes, shows a high-spin gs for large J_1/J_2 in the thermodynamic limit. Thomas *et al.* showed that fused azulene systems have both a high-spin gs and permanent electric polarization in the thermodynamic limit [62]. In addition, it is possible to fabricate such ladders as defects in graphene layers or at the grain boundaries in graphene [63–65]. The electrons in the $2p_z$ orbital of the carbon atoms in these ladders form a strongly correlated band that can be modeled by a long-range interacting model such as the Pariser-Parr-Pople (PPP) model [66]. The PPP model transforms into an isotropic spin-1/2 Heisenberg model with antiferromagnetic exchange interactions. The magnetic properties of these two models are closely related [62]. The behavior of these systems in the presence of a static axial magnetic field had not been studied so far. Here, we analyze the behavior of this skewed ladder in the presence of an external magnetic field.

The skewed ladders can be of various types [61], but in this paper we study only the 5/7 skewed ladder shown in Fig. 1(b). In this system there are eight spins and ten bonds per unit cell. There are two bonds with exchange interaction J_1 and eight bonds with J_2. This system shows a high-spin gs in the large J_1 ($>2.35J_2$) limit, and one-quarter of the spins in each unit cell are connected through the effective ferromagnetic interaction while the remaining six spins form three singlet dimers [61]. The OYA condition predicts the possibility of plateaus at $m = 0$, 1/4, 1/2, and 3/4 for this system. In this paper, we show that there are indeed three plateaus at $m = 1/4$, 1/2, and 3/4 in the 5/7 skewed ladder system; in the regular zigzag chain a lone plateau at $m = 1/3$ is observed, although the OYA condition predicts two more plateaus at $m = 0$ and 2/3 [18,23,24]. These plateaus in the 5/7 ladder are formed because of the strong dimer formations in the system. The existence of four plateaus in a ladder is not found in the literature. We also explore the cusp at the ends of the plateaus.

This paper is divided into four sections. In Sec. II we discuss the model Hamiltonian and the numerical method. The results are presented in Sec. III, which has three subsections. A discussion of the results is presented in Sec. IV.

II. MODEL AND METHOD

In Fig. 1(b) we show schematically a 5/7 ladder. All exchange interactions between the spins are antiferromagnetic in nature. The sites are numbered such that odd-numbered sites are on the bottom leg and even-numbered sites are on the top leg. In this scheme, the rung bonds are the nearest-neighbor exchanges J_1 and the bonds on the legs are the next-nearest-neighbor exchanges. The nearest-neighbor exchange J_1 is taken in units of J_2, which defines the energy scale. In the presence of an axial magnetic field B, the model Hamiltonian can be written as

$$H_{5/7} = J_1 \sum_{i=0}^{n} (\vec{S}_{8i+1} \cdot \vec{S}_{8i+2} + \vec{S}_{8i+4} \cdot \vec{S}_{8i+5}) + J_2 \sum_{i=0}^{n} \sum_{k=1}^{8} \vec{S}_{8i+k} \cdot \vec{S}_{8i+k+2} - B \sum_{i=0}^{n} \sum_{k=1}^{8} S^z_{8i+k}, \quad (1)$$

where i labels the unit cell and k is the spin in the unit cell, as shown in Fig. 1(b). The first and second terms denote the rung exchange interaction J_1 and the interaction along the legs J_2, and the third term of the Hamiltonian gives the interaction of the spins with an axial field B in units of $J_2/g\mu_B$.

The Hamiltonian in Eq. (1) is many-body in nature, therefore we need to deal with a large number of degrees of freedom. We use the density matrix renormalization group (DMRG) method to handle the large degrees of freedom [67–69]. The DMRG method is based on systematic truncation of irrelevant degrees of freedom. The dimension of the chosen effective density matrix m (which is also the number of block states, not to be confused with fractional magnetization) varies by up to 400, and the truncation error of the density matrix is less than 10^{-11}. We also carry out five to six finite DMRG sweeps for satisfactory convergence of the eigenstate. The growth sequence of the system is the same as that in our earlier work [61]. The lowest eigenstates in all M_S sectors, from zero to $N/2$, are calculated to find the total spin S_{gs} of the gs from the condition $E_0(S_{gs} - 1) = E_0(S_{gs}) < E_0(S_{gs} + 1)$. An exact diagonalization (ED) technique is used to calculate the gs properties of small systems.

III. RESULTS AND DISCUSSIONS

The 5/7 ladder system has eight spins per unit cell, and in the large-J_1 limit the ground state can be represented as six spins forming three singlet dimers and weak ferromagnetic interaction between the remaining two spins on the same legs in the two adjacent rings. Therefore, in the thermodynamic limit, for $J_1/J_2 > 2.35$, the magnetization in the gs is $m = 1/4$. In the strong J_1 (> 2.35) limit, the gs has $m = 1/4$ for $B = 0$, even for small systems. In this paper, we focus on the gs properties in the presence of an axial magnetic field, and we show that there are three plateau phases at $m = 1/4$, 1/2, and 3/4 as predicted by the generalized Lieb-Schultz-Mattis theorem [25,36,59]. To understand the plateau phases, we analyze the gs energies, spin densities, and spin-spin correlations in the presence of the applied magnetic field, B. The Hamiltonian in Eq. (1) conserves M_S, therefore field-dependent gs energies are obtained simply by adding the Zeeman term to the zero-

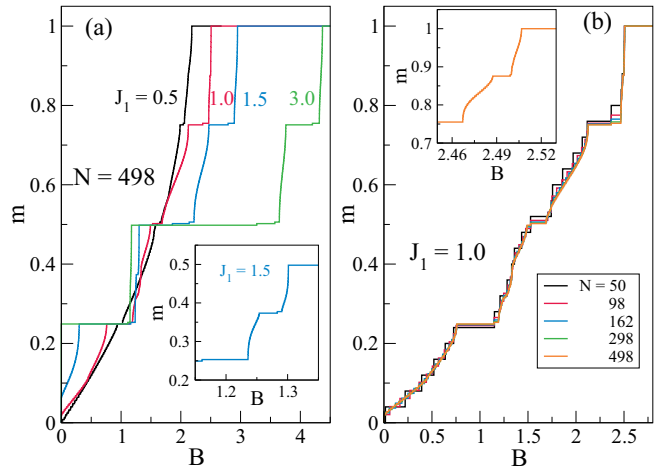

FIG. 2. (a) m-B curve for a 5/7 skewed ladder for $J_1 = 0.5$, 1.0, 1.5, and 3.0 for $N = 498$ sites. The inset shows an $m = 3/8$ plateau for $J_1 = 1.5$. (b) The finite-size effect of the m-B curve with $J_1 = 1.0$ for five system sizes. The inset shows an $m = 7/8$ plateau at this J_1 value.

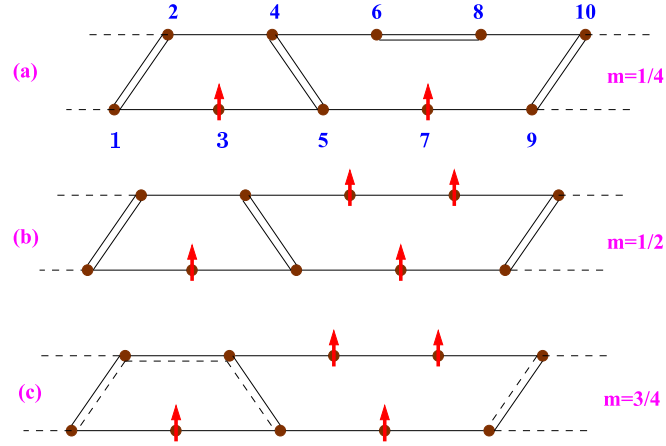

FIG. 3. Schematic representation of the gs in terms of singlet dimers and aligned free spins at (a) $m = 1/4$ plateau, (b) $m = 1/2$ plateau, and (c) $m = 3/4$ plateau, where broken lines imply a triplet delocalized over four sites.

field energies,

$$E(M_S, B) = E_0(M_S, B = 0) - BM_S, \tag{2}$$

where M_S is the z-component of the total spin. The change in magnetization from M_S to M'_S occurs at the crossing of the $E(M_S, B)$ and $E(M'_S, B)$ lines.

The gs of this model was studied in the absence of a magnetic field in Ref. [61], and it shows a high-spin ferrimagnetic gs even at $J_1 = 1$ and a reentrant antiferromagnetic phase for $1.75 < J_1 < 2.18$. The gs has $S = n$ (the number of unit cells) for $J_1 > 2.35$. In this phase, the spins at sites 3, 7, 11, ... have effective ferromagnetic interactions [61]. The spin density ρ_i at site i and axial spin correlation $C(r)$ between spins at sites i and $i + r$ are defined as

$$\rho_i = \langle \text{gs} \mid S_i^z \mid \text{gs} \rangle,$$
$$C(r) = \langle \text{gs} \mid S_i^z S_{i+r}^z \mid \text{gs} \rangle. \tag{3}$$

The results are presented in the following four subsections. First the m-B curves and their corresponding energies are presented in Sec. III A. To understand all three plateau phases, the spin density ρ_i at site "i" and the spin-spin correlation function $C(r)$ [Eq. (3)] are studied for different M_S values in Sec. III B. From these we can infer the gs spin configurations at different magnetization plateaus. Here we also study the cusp singularities and thermal stability of plateaus. The analytical perturbation theory to support this is discussed in Sec. III C.

A. Plateau phases in a 5/7 ladder

We plot the m-B curve for different strengths of the rung exchange J_1 in Fig. 2 for $N = 498$ spins (62 unit cells), and we note that the $m = 1/4$ and 3/4 plateaus appear for $J_1 \geqslant 0.4$, whereas the other plateau at $m = 1/2$ appears for $J_1 \geqslant 0.9$. Let us define B_i^L and B_i^U as the lower and upper critical values of the magnetic field for the ith plateau, where $i = 1$, 2, and 3 for the three plateaus at $m = 1/4$, 1/2, and 3/4, respectively. We note that the onset field of the first plateau at $m = 1/4$ decreases as J_1 increases, while the width of the plateau $w_1 = (B_1^U - B_1^L)$ increases with increasing J_1. The width of the 1/4 plateau increases linearly with J_2 in the large-J_1 limit, as shown analytically in Sec. III C. We notice that a finite field is required to reach $m = 1/4$ for small J_1; in this limit of J_1, the rung dimers are weak and a finite field is required to align spins 3 and 7 in the field direction. In the $J_1 > 2.35$ limit, all the rung singlets are strong, and an effective ferromagnetic interaction develops between spin 3 and 7 as shown in Fig. 3(a). Thus the field required to attain the 1/4 plateau decreases to zero. Along both legs, most bonds are weak except the generic 6-8 bond in each unit cell. Therefore, the next plateau occurs when the 6-8 bond breaks and the system enters another locked phase with $m = 1/2$ [Fig. 3(b)]. In this case, most of the magnetic contribution comes from the ferromagnetically aligned spins at sites 3, 6, 7, and 8 in the unit cell [Fig. 3(b)]. On further ramping the field B, the singlet involving sites 1, 2, 4, and 5 flips to yield a triplet, and the system locks into the $m = 3/4$ plateau phase [Fig. 3(c)]. At fields greater than the saturation field B_{sat}, all singlet bonds in every unit cell are broken, and the system goes to a completely polarized state.

Other than these three significant plateaus, there is a narrow plateau at $m = 3/8$ for $1.2 < J_1 < 2.5$ and another at $m = 7/8$ for $J_1 = 1.0$, as shown in the insets of Figs. 2(a) and 2(b), respectively. These plateaus disappear at larger J_1 values. In the OYA condition, if we consider an enlarged unit cell of $p = 16$ sites, then there is the possibility of plateaus at $m = 1/8$, 3/8, 5/8, and 7/8 other than the plateaus mentioned earlier. However, we only find two of them, namely at $m = 3/8$ and 7/8 for a particular range of J_1 values. Again we can conjecture that the $m = 3/8$ plateau appears because at the corresponding magnetic field one of the singlet bonds 6-8 or 14-16 [Fig. 1(b)] in the enlarged unit cell breaks. Similarly, the $m = 7/8$ plateau could arise when one of the triplets involving sites [1,2,4,5] or [9,10,12,13] leads to four unpaired spins. At large $J_1 > 2.5$, these small plateaus disappear, perhaps

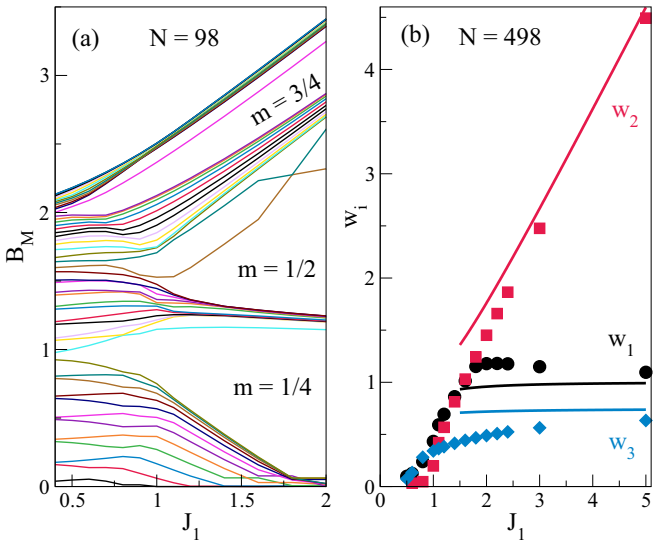

FIG. 4. (a) The magnetic field B_M required to close the energy gap between successive lowest energy M_S states vs the strength of nearest-neighbor exchange J_1. B_M is in units of $J_2/g\mu_B$. The M values increase from $M = 1$ for the bottom curve to $M = 49$ for the uppermost curve. At large J_1, these curves collapse into four groups with $m = M/M_{\max} = 1/4$, $1/2$, $3/4$, and 1. (b) The width of the plateaus w_1, w_2, and w_3 for $m = 1/4$, $1/2$, and $3/4$ plotted as a function of J_1 for a system with $N = 498$ spins. The solid lines are the plateau widths calculated from the perturbation theory in the large-J_1 limit (see Sec. III C).

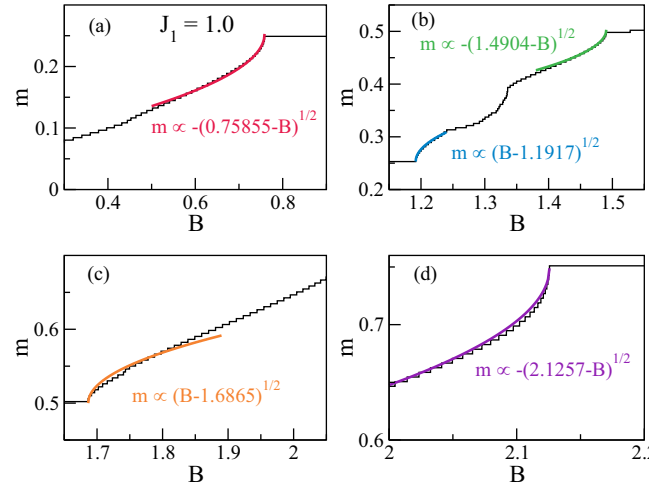

FIG. 5. Behavior of magnetization at the plateau ends for a 5/7 ladder at $J_1 = J_2 = 1.0$ for $N = 498$ spins (62 unit cells) (a) $m = 1/4$ plateau at B_c^L, (b) $m = 1/4$ plateau at B_c^U, (c) $m = 1/2$ plateau at B_c^U, and (d) 3/4 plateau at B_c^L. The magnetization near the plateaus obeys $\propto (B - B_c)^{1/2}$, and the numerical m vs B dependence at the plateau ends is shown in the figure.

because the correlations become short-ranged and the coupling between unit cells becomes weak.

To estimate the width of the plateaus, we plot the magnetic field, B, required to achieve successively higher M_S states for a given J_1. Here, we define the magnetic field B_M as the magnetic field required to close the gap between the $M_S = M$ and $M_S = M + 1$ state, i.e.,

$$B_M = \frac{E_0(M+1) - E_0(M)}{g\mu_B}. \tag{4}$$

In Fig. 4(a) we notice that the B_M curves collapse into four bands for large J_1: the first band corresponds to $m = 1/4$, the second corresponds to $m = 1/2$, the third corresponds to $m = 3/4$, and the fourth corresponds to $m = 1$. This is a consequence of the fact that for large J_1, the ground state has a spin $p/8$, and excited states with a finite gap in the thermodynamic limit have spins $p/4$, $3p/8$, and $p/2$, where p is the number of spins in a unit cell. There are three plateaus of significance corresponding to $m = 1/4$, $1/2$, and $3/4$. The width of the $1/4$ plateau at large J_1 corresponds to the magnetic-field difference between the $m = 1/4$ and $1/2$ bands. This remains independent of J_1 at large J_1. The magnetic field B_M for $m = 1/2$ is independent of J_1 while that of B_M with $m = 3/4$ increases linearly with J_1 at large J_1. Therefore in this limit, the plateau width for $m = 1/2$ increases linearly with J_1. The width of the $m = 3/4$ plateau is independent of J_1 as the B_M for $m = 3/4$ and 1 both increase linearly with J_1 and their difference is independent of J_1 for large J_1. This can be seen in Fig. 4(b), where the plateau width for magnetization calculation is plotted as a function of J_1.

At the ends of the plateaus, the magnetization should vary as $m(B) - m(B_c) \propto (B - B_c)^{1/2}$ [70], where B_c is the magnetic field at the end of the plateau under consideration. In fact for a 5/7 ladder, there are at least four cusp singularities (at $m = 1/4$, $1/2$, and $3/4$) in the m-B curve for the $J_1 = 1$ case with $N = 498$ spins (62 unit cells) as shown in Fig. 5. The magnetization curves near the plateau are fitted with $m \propto (B - B_c)^{1/2}$. The B_c^L (B_c^U) for this system for $J_1 = 1$ are 0.759 (1.192), 1.490 (1.687), and 2.126 for $m = 1/4$, $1/2$, and $3/4$, respectively (Fig. 5). At $J_1 = 1.0$ in Fig. 5(b), we also see a cusplike behavior for $m \approx 0.31$ and ≈ 0.39. This corresponds to viewing the spin system as belonging to a larger unit cell, as near those values the onset of new plateaus occurs, assuming a larger magnetic unit cell.

For sufficiently large J_1, the plateaus are wide and the energy gap near each plateau is large. Any practical application of these plateaus is feasible only if they are stable to thermal fluctuations. The finite-temperature behavior of the magnetization plateau of the system is shown in Fig. 6(a) with $J_1 = 1.6$ for $N = 98$ spins. We have used a hybrid ED-DMRG method with the average density matrix taken over many states in each M_S sector [71]. We have used 300 energy eigenvalues from each M_S sector for thermal averaging of the magnetization. Since we are focusing on the low-temperature properties of the system, retaining 300 low-lying states in each M_S sector should be accurate as higher excited states are practically inaccessible at low temperatures. As shown in Fig. 6(a), the plateaus at $m = 1/4$ and $1/2$ are robust at finite temperatures, while the plateau at $3/4$ survives only up to $T/J_2 = 0.05$. The derivative $\chi = \frac{dm}{dB}$ versus B is shown in Fig. 6(b). In the plateau regime, the susceptibility χ vanishes at $T = 0$, whereas it is finite when the plateaus are perturbed by the thermal fluctuations. We notice that the $3/4$ plateau is very much susceptible to the thermal fluctuation as χ is finite even at low temperatures, however $m = 1/4$ and $1/2$

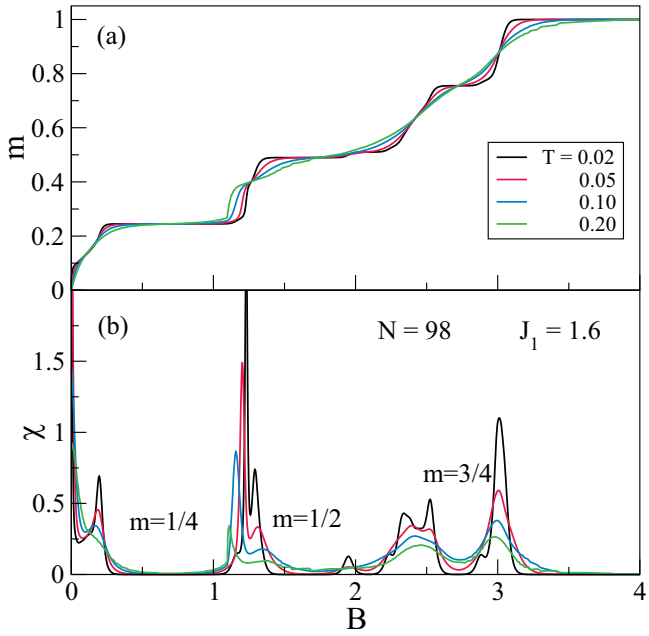

FIG. 6. m-B curve at four temperatures $T/J_2 = 0.02$, 0.05, 0.10, and 0.20 for $J_1 = 1.60$ and $N = 98$ spins.

plateaus survive thermal fluctuations. This can be attributed to small energy gaps between the successive lowest M_S states near the $m = 3/4$ plateau, which leads to a gradual change in magnetization at low temperatures. We also note that the plateau width is smallest for the $m = 3/4$ plateau at 0 K, which also implies that the plateau should disappear on slight warming.

B. Spin density and correlation function in the plateau phase

To identify the spins that are aligned along the applied field in a given plateau, we study the spin densities and spin-spin correlation functions with 24 spins under a periodic boundary condition (PBC). For a system of 24 spins, M_S varies from 0 to 12. We obtain spin densities at all the sites for the lowest eigenstate in each positive M_S sector. Based on the calculated spin densities, we find that sites (1, 5), (2, 4), (3, 7), and (6, 8) have very nearly the same spin densities in all the M_S sectors of the system. We show in Fig. 7 the variation of spin densities with $m = M_S/12$ for $J_1 = 1.8$ and 5.0 corresponding to below and above the critical rung interaction $J_{1c} = 2.35$.

The spin densities at site numbers 3 and 7 increase quickly with m, which attains the value $\rho_3 \simeq \rho_7 \sim 0.5$ at $m = 1/4$ for both $J_1 = 1.8$ and 5.0. In fact, for large values of $J_1 > 2.35$, ρ_3 and ρ_7 are both 0.5 without any field as $m = 1/4$ is the gs. The spin densities at 6 and 8 (ρ_6 and ρ_8) increase linearly with m between $m = 1/4$ and 1/2, and these go to 0.5 for $M_S = 6$. At the magnetic field at which this state becomes the gs, the 6-8 singlet bond breaks and becomes a triplet bond. The spins at the remaining sites, namely 1, 2, 4, and 5, form a singlet and have very low spin densities. This singlet state transitions to a triplet for the $m = 3/4$ plateau, and the gs has $M_S = 9$. In this state, the singlet formed by the spins 1, 2, 4, and 5 is canted to a triplet while the spins at other sites are ferromagnetically aligned. Hence, the spin

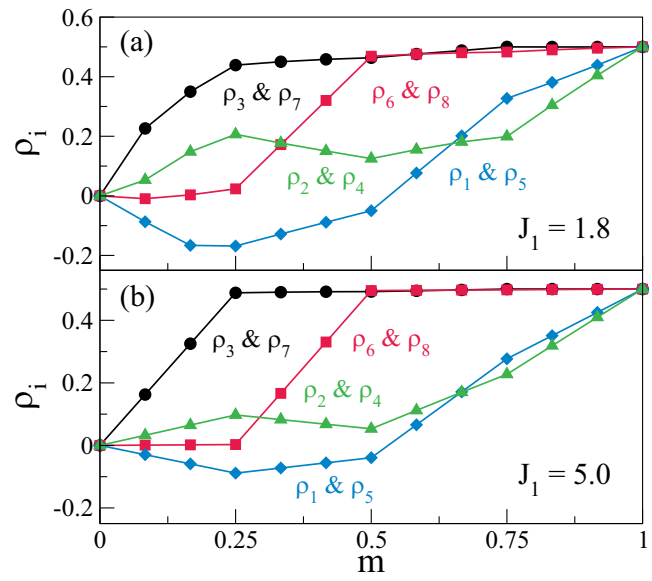

FIG. 7. The spin densities at different sites in a unit cell of a 5/7 ladder of $N = 24$ sites with a periodic boundary condition.

densities ρ_1, ρ_2, ρ_4, and ρ_5 are almost equal beyond $m = 0.75$. To understand the effective interactions between the neighboring spins, we study the bond energies or magnetic bond order $b_{i,j} = -\langle \psi_{\rm gs} \mid \vec{S}_i \cdot \vec{S}_j - \frac{1}{4} \mid \psi_{\rm gs} \rangle$, where the sites i and j are connected either by a J_1 or a J_2 interaction. There are ten such bonds in a unit cell, and we show only dominant bond-orders in a unit cell in Fig. 8. Only the bonds (1, 2), (4, 5), (6, 8), and (2, 4) are significant, and others are small and increase with m. We find $b_{12} = b_{45}$ and $b_{13} = b_{35}$ for all M_S values. For degenerate states we obtained b_{ij} by diagonalizing the

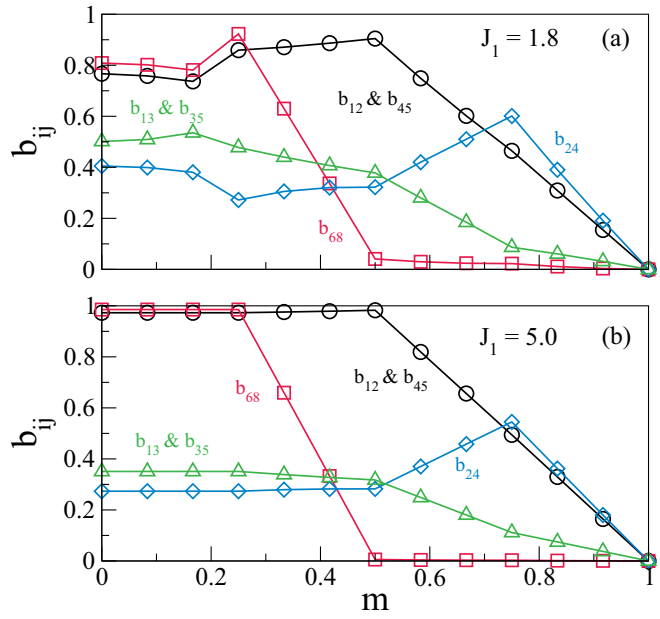

FIG. 8. The bond energies or the bond order for different bonds in a unit cell of a 5/7 ladder of $N = 24$ sites with a periodic boundary condition.

bond-order matrix in the basis of degenerate states. In Fig. 8, we show the variation of b_{ij} with m. In the large-J_1 case, we note that for $m = 1/4$, the (6, 8), (1, 2), and (4, 5) bonds are singlets. The (1, 3), (3, 5), and (2, 4) bonds are weak and have a large triplet component. The (3, 7) bond (not shown in the figure) always remains a triplet. When m reaches the value of 0.5, the (6, 8) singlet breaks and a triplet is obtained. This is true even for small J_1 [Fig. 8(a)]. As the m value increases further, (1, 2) and (4, 5) bonds resonate between a singlet and a triplet, but the (2, 4) bond becomes a singlet. This can be represented as a state in which resonance involves the valence bond pairing $[1, 2](4, 5) \leftrightarrow [2, 4](1, 5) \leftrightarrow (1, 2)[4, 5]$, where square brackets imply singlet pairing and parentheses imply triplet pairing of spins at sites indicated inside the parentheses. All the singlet bonds are broken when $m = 1$, as is to be expected.

C. Perturbation calculations for plateau phases

The numerical studies indicate that we can develop an understanding of the plateau phases from a perturbative approach in the large-J_1 limit. Hence, we treat the J_2 terms in the spin Hamiltonian as a perturbation over the J_1 terms. Within a unit cell, the J_1 term provides interactions between spins S_1 and S_2, and S_4 and S_5, while the J_2 term operates between spin pairs S_2, S_4; S_4, S_6; S_6, S_8; S_1, S_3; S_3, S_5; and S_5, S_7. Since the spins S_6 and S_8 experience only J_2 interaction, we include this interaction also in the unperturbed Hamiltonian. Thus for a perturbation calculation, the zeroth-order Hamiltonian over one unit cell under a periodic boundary condition is given by

$$H_0 = J_1(\vec{S}_1 \cdot \vec{S}_2 + \vec{S}_4 \cdot \vec{S}_5) + J_2 \vec{S}_6 \cdot \vec{S}_8 - B\big(S_3^z + S_7^z\big). \quad (5)$$

Other terms of the Hamiltonian involve J_2 interaction and can be treated as perturbation H_1 given by

$$H_1 = J_2 \sum_{k=1}^{8} \vec{S}_k \cdot \vec{S}_{k+2} - J_2 \vec{S}_6 \cdot \vec{S}_8 - B\big(S_{\rm tot}^z - S_3^z - S_7^z\big), \quad (6)$$

where a cyclic boundary condition is implied in the summation. The ground state of the unperturbed system in terms of the spin couplings can be written as

$$|\psi_0\rangle = |\overline{1\ \ 2}\ \uparrow_3\ \overline{4\ \ 5}\ \ \widehat{6\uparrow_7 8}\rangle. \quad (7)$$

In Eq. (7), the convention we follow is $|\overline{i\ \ j}\rangle = \frac{1}{\sqrt{2}}\{|\uparrow_i\downarrow_j\rangle - |\downarrow_i\uparrow_j\rangle\}$. The zeroth-order energy of the system can be obtained by operating the zeroth-order Hamiltonian H_0 on the state $|\psi_0\rangle$ in Eq. (7), and it is given by

$$\mathcal{E}_0 = -\tfrac{3}{2}J_1 - \tfrac{3}{4}J_2 - B. \quad (8)$$

The first-order contribution from H_1 vanishes as the matrix elements $\langle\psi_0 \mid H_1 \mid \psi_0\rangle = 0$. The second-order correction to the energy is given by

$$E^{(2)} = \sum_{\rm ex} \frac{|\langle\psi_{\rm ex}|H_1|\psi_0\rangle|^2}{\mathcal{E}_{\rm ex}^{(0)} - \mathcal{E}_{\rm gs}^{(0)}}. \quad (9)$$

We can obtain the excited states that connect to the ground states $|\psi_0\rangle$ by operating each term in H_1 on $|\psi_0\rangle$; the resulting state will be an excited state of H_0, whose unperturbed energy is computed by acting on this resulting $|\psi_{\rm ex}\rangle$ by H_0. For example, consider the first exchange interaction term in H_1, which is $J_2(\vec{S}_1 \cdot \vec{S}_3)$. When this operates on $|\psi_0\rangle$, we get the state

$$J_2(\vec{S}_1 \cdot \vec{S}_3)|\psi_0\rangle = -\frac{J_2}{2\sqrt{2}}|\psi_{\rm ex}\rangle = -\frac{1}{2\sqrt{2}}|\uparrow_1\uparrow_2\downarrow_3\ \overline{4\ \ 5}\ \ \widehat{6\uparrow_7 8}\rangle. \quad (10)$$

The unperturbed energy of the $|\psi_{\rm ex}\rangle$, $\mathcal{E}_{\rm ex}^{(0)}$ is given by $-\frac{J_1}{2} - \frac{3}{4}J_2 - B$. Similarly, we can calculate the matrix elements of other exchange operators occurring in H_1 on the basis of the eigenstates of H_0. This gives the second-order corrected energy of the ground state of H_0 as

$$\mathcal{E}_{\rm gs}^{(2)} = -\frac{3J_1}{2} - \frac{3J_2}{4} - \frac{9J_2^2}{16J_1} - \frac{J_2^2}{4(J_1+J_2)} - B. \quad (11)$$

Exact diagonalization of the skewed ladder Hamiltonian of 24 sites for $J_1 = 5.0$ and $J_2 = 1.0$ gives a per site energy of -1.067 as compared with the perturbation theory prediction of -1.05 corresponding to an error of $\sim$1.6%. Similarly the exact and second-order corrected ground-state energy per site from perturbation theory for $J_1 = 2.5$ and $J_2 = 1.0$ is -0.63 and -0.60, respectively. Thus the error in perturbation theory is less than 5.0% in this case as well.

Our numerical results show that the next plateau occurs at $m = 1/2$, corresponding to the breaking of the (6, 8) singlet bond. The eigenstate of the unperturbed Hamiltonian in this case is $|\overline{1\ \ 2}\ \uparrow_3\ \overline{4\ \ 5}\ \uparrow_6\uparrow_7\uparrow_8\rangle$. The energy of the state correct to second order in perturbation is given by

$$\mathcal{E}_{m=1/2}^{(2)} = -\frac{3J_1}{2} + \frac{J_2}{4} - \frac{13J_2^2}{16J_1} - 2B. \quad (12)$$

The error in energy per site of perturbation theory compared with exact results for 24 sites in the absence of an applied magnetic field is $< 0.5\%$ for $J_1 = 5.0$ and $< 0.6\%$ for $J_1 = 2.5$. From our numerical studies, the ground state with $m = 3/4$ is obtained by creating a triplet superposition of the two states formed by nearest-neighbor singlets and triplets from spins at sites 1, 2, 4, and 5 while all other spins have $m_S = +1/2$ in the unit cell. Thus we consider the $|\psi_{m=3/4}^{(0)}\rangle$ as given by

$$\big|\psi_{m=3/4}^{(0)}\big\rangle = \frac{1}{\sqrt{2}}[|\overline{1\ \ 2}\ \uparrow_3\overrightarrow{4\ \ 5}\ \uparrow_6\uparrow_7\uparrow_8\rangle + |\overrightarrow{1\ \ 2}\ \uparrow_3\overline{4\ \ 5}\ \uparrow_6\uparrow_7\uparrow_8\rangle], \quad (13)$$

where $|\overrightarrow{i\ \ j}\rangle$ corresponds to $|\uparrow_i\uparrow_j\rangle$, which is an $M_S = 1$ triplet. Using this as the unperturbed state, we can obtain the ground-state energy of the unit cell in the $m = 3/4$ state as

$$\mathcal{E}_{m=3/4}^{(2)} = -\frac{J_1}{2} + \frac{3J_2}{4} - \frac{3J_2^2}{8J_1} - 3B. \quad (14)$$

This again has an error of $\sim$1% for $J_1 = 5.0$ and $< 5\%$ for $J_1 = 2.5$ when compared with exact diagonalization results for the 24-site skewed ladder under a periodic boundary condition in zero external field. In the fully polarized case, which corresponds to

$$\big|\psi_{m=1}^{(0)}\big\rangle = |\uparrow_1\uparrow_2\uparrow_3\uparrow_4\uparrow_5\uparrow_6\uparrow_7\uparrow_8\rangle, \quad (15)$$

the exact energy is trivially given by

$$\mathcal{E}_{m=1} = \frac{J_1}{2} + 2J_2 - 4B. \tag{16}$$

From the perturbation calculation, we obtain the critical fields for the onset of the plateaus at $m = 1/2$, $3/4$, and 1, which also correspond to the end of $m = 1/4$, $1/2$, and $3/4$ plateaus. The onset magnetic field for the first plateau, B_{c_1}, is obtained when the ground state with $m = 1/4$ becomes degenerate with the lowest-energy state with $m = 1/2$. Thus, by equating the right-hand side of Eqs. (11) and (12), we get

$$B_{c_1} = J_2 - \frac{J_2^2}{4J_1} + \frac{J_2^2}{4(J_1 + J_2)}. \tag{17}$$

Similarly, by equating the right-hand side of Eqs. (12) and (14) we get B_{c_2}, and by equating the right-hand side of Eqs. (14) and (16) we get B_{c_3} as

$$B_{c_2} = J_1 + \frac{1}{2}J_2 + \frac{7J_2^2}{16J_1}, \tag{18}$$

$$B_{c_3} = J_1 + \frac{5}{4}J_2 + \frac{3J_2^2}{8J_1}. \tag{19}$$

From these critical fields, we calculate the plateau widths as $w_1 = B_{c_1}$, $w_2 = B_{c_2} - B_{c_1}$, and $w_2 = B_{c_3} - B_{c_2}$. These plateau widths are in good agreement with the numerical results, as seen in Fig. 4(b), for $J_1 > 1.5$.

IV. SUMMARY

In this paper, we have studied the magnetic properties of an antiferromagnetically interacting spin-1/2 system arranged on a 5/7 skewed ladder lattice [Fig. 1(b)]. This system shows a high-spin gs with $m = 1/4$ even in the absence of a magnetic field B for $J_1 > 2.35$ [61]; J_1 is the rung interaction, while the interaction between the nearest neighbors on the leg J_2 is set to 1. This ladder system is also interesting and unique as it exhibits many plateaus. We have obtained the m-B curve, and we find that there are three magnetization plateaus as a function of B. These three plateaus are at $m = 1/4$, $1/2$, and $3/4$, consistent with the OYA condition. In the gs at $B = 0$, each unit cell has three singlet dimers and two ferromagnetically arranged free spins [Fig. 3(a)]. We find that each plateau formation corresponds to successive breaking of a singlet dimer (Fig. 3). We have analytically obtained the widths of these plateaus as a function of J_1 from a simple perturbation theory.

The plateaus at $m = 1/4$ and $3/4$ appear even for small J_1 (> 0.4), but the $m = 1/2$ plateau appears only for $J_1 > 0.8$. The width w_i of the ith plateau at m_i represents the magnitude of the energy gap in the system for that particular magnetization. We notice that w_i always increases with J_1; however, for $m = 1/4$ and $1/2$ it depends weakly on J_1, and at $m = 3/4$ the plateau width exhibits an almost linear variation with J_1. This is consistent with the perturbation theory results. As usual, this system also shows cusps in the m-B curve at the beginning and end of the plateaus, and it follows the square root dependence, $m \propto (B - B_c)^{1/2}$. The stability of the magnetization plateaus in the presence of thermal fluctuation is an important factor for its observation. We notice that the plateaus at $m = 1/4$ and $1/2$ are robust against small thermal fluctuation, while the plateau at $3/4$ survives only up to $T/J_2 = 0.05$. The skewed ladder system can be mapped to a molecular system corresponding to fused five- and seven-membered carbon rings [62]. Such a system corresponds to a fused azulene lattice [62], and it may be engineered at the grain boundary of a graphene sheet [63–65].

ACKNOWLEDGMENTS

M.K. thanks Department of Science and Technology (DST), India for a Ramanujan fellowship. S.R. gratefully acknowledges INSA Senior Scientist and a DST-SERB grant.

D.D. and S.D. contributed equally to this work.

[1] C. K. Majumdar and D. K. Ghosh, J. Math. Phys. **10**, 1388 (1969); **10**, 1399 (1969).
[2] T. Hamada, J.-i. Kane, S.-i. Nakagawa, and Y. Natsume, J. Phys. Soc. Jpn. **57**, 1891 (1988).
[3] A. V. Chubukov, Phys. Rev. B **44**, 4693 (1991).
[4] R. Chitra, S. Pati, H. R. Krishnamurthy, D. Sen, and S. Ramasesha, Phys. Rev. B **52**, 6581 (1995).
[5] S. R. White and I. Affleck, Phys. Rev. B **54**, 9862 (1996).
[6] C. Itoi and S. Qin, Phys. Rev. B **63**, 224423 (2001).
[7] S. Mahdavifar, J. Phys.: Condens. Matter **20**, 335230 (2008).
[8] J. Sirker, Phys. Rev. B **81**, 014419 (2010).
[9] M. Kumar, A. Parvej, and Z. G. Soos, J. Phys.: Condens. Matter **27**, 316001 (2015).
[10] Z. G. Soos, A. Parvej, and M. Kumar, J. Phys.: Condens. Matter **28**, 175603 (2016).
[11] M. Kumar, S. Ramasesha, and Z. G. Soos, Phys. Rev. B **81**, 054413 (2010).
[12] M. Kumar and Z. G. Soos, Phys. Rev. B **85**, 144415 (2012).
[13] T. Vekua, A. Honecker, H.-J. Mikeska, and F. Heidrich-Meisner, Phys. Rev. B **76**, 174420 (2007).
[14] T. Hikihara, L. Kecke, T. Momoi, and A. Furusaki, Phys. Rev. B **78**, 144404 (2008).
[15] J. Sudan, A. Lüscher, and A. M. Läuchli, Phys. Rev. B **80**, 140402(R) (2009).
[16] D. V. Dmitriev and V. Y. Krivnov, Phys. Rev. B **77**, 024401 (2008).
[17] F. Heidrich-Meisner, A. Honecker, and T. Vekua, Phys. Rev. B **74**, 020403(R) (2006).
[18] F. Heidrich-Meisner, I. A. Sergienko, A. E. Feiguin, and E. R. Dagotto, Phys. Rev. B **75**, 064413 (2007).
[19] F. Heidrich-Meisner, I. P. McCulloch, and A. K. Kolezhuk, Phys. Rev. B **80**, 144417 (2009).
[20] A. Parvej and M. Kumar, Phys. Rev. B **96**, 054413 (2017).
[21] L. Kecke, T. Momoi, and A. Furusaki, Phys. Rev. B **76**, 060407(R) (2007).
[22] A. Parvej and M. Kumar, J. Magn. Magn. Mater. **401**, 96 (2016).

[23] K. Tandon, S. Lal, S. K. Pati, S. Ramasesha, and D. Sen, Phys. Rev. B **59**, 396 (1999).

[24] K. Okunishi and T. Tonegawa, Phys. Rev. B **68**, 224422 (2003); J. Phys. Soc. Jpn. **72**, 479 (2003).

[25] M. Oshikawa, M. Yamanaka, and I. Affleck, Phys. Rev. Lett. **78**, 1984 (1997).

[26] D. C. Cabra, A. Honecker, and P. Pujol, Phys. Rev. Lett. **79**, 5126 (1997).

[27] K. Totsuka, Phys. Rev. B **57**, 3454 (1998).

[28] T. Sakai and M. Takahashi, Phys. Rev. B **57**, R3201 (1998).

[29] T. Sakai and S. Yamamoto, Phys. Rev. B **60**, 4053 (1999).

[30] A. Honecker, F. Mila, and M. Troyer, Eur. Phys. J. B **15**, 227 (2000).

[31] K. Okamoto, N. Okazaki, and T. Sakai, J. Phys. Soc. Jpn. **70**, 636 (2001).

[32] K. Hida and I. Affleck, J. Phys. Soc. Jpn. **74**, 1849 (2005).

[33] J. Alicea and M. P. A. Fisher, Phys. Rev. B **75**, 144411 (2007).

[34] F. D. M. Haldane, Phys. Lett. A **93**, 464 (1983).

[35] F. D. M. Haldane, Phys. Rev. Lett. **50**, 1153 (1983).

[36] I. Affleck and E. H. Lieb, Lett. Math. Phys. **12**, 57 (1986).

[37] H. Nakano and M. Takahashi, J. Phys. Soc. Jpn. **67**, 1126 (1998).

[38] K. Morita, T. Sugimoto, S. Sota, and T. Tohyama, Phys. Rev. B **97**, 014412 (2018).

[39] J. Schulenburg, A. Honecker, J. Schnack, J. Richter, and H.-J. Schmidt, Phys. Rev. Lett. **88**, 167207 (2002).

[40] H.-J. Schmidt, J. Richter, and R. Moessner, J. Phys. A **39**, 10673 (2006).

[41] S. Nishimoto, N. Shibata, and C. Hotta, Nat. Commun. **4**, 2287 (2013).

[42] S. Capponi, O. Derzhko, A. Honecker, A. M. Läuchli, and J. Richter, Phys. Rev. B **88**, 144416 (2013).

[43] S. Pal, A. Mukherjee, and S. Lal, J. Phys.: Condens. Matter **32**, 165805 (2020).

[44] D. J. J. Farnell, R. Zinke, J. Schulenburg, and J. Richter, J. Phys.: Condens. Matter **21**, 406002 (2009).

[45] H. Kikuchi, Y. Fujii, M. Chiba, S. Mitsudo, T. Idehara, T. Tonegawa, K. Okamoto, T. Sakai, T. Kuwai, and H. Ohta, Phys. Rev. Lett. **94**, 227201 (2005).

[46] H. Kikuchi, Y. Fujii, M. Chiba, S. Mitsudo, T. Idehara, T. Tonegawa, K. Okamoto, T. Sakai, T. Kuwai, and H. Ohta, Phys. Rev. Lett. **97**, 089702 (2006).

[47] B. Gu and G. Su, Phys. Rev. Lett. **97**, 089701 (2006).

[48] M. Hase, M. Kohno, H. Kitazawa, N. Tsujii, O. Suzuki, K. Ozawa, G. Kido, M. Imai, and X. Hu, Phys. Rev. B **73**, 104419 (2006).

[49] Y. Zhao, S.-S. Gong, W. Li, and G. Su, Appl. Phys. Lett. **96**, 162503 (2010).

[50] A. Maignan, V. Hardy, S. Hébert, M. Drillon, M. R. Lees, O. Petrenko, D. M. K. Paul, and D. Khomskii, J. Mater. Chem. **14**, 1231 (2004).

[51] V. Hardy, D. Flahaut, M. R. Lees, and O. A. Petrenko, Phys. Rev. B **70**, 214439 (2004).

[52] X. X. Wang, J. J. Li, Y. G. Shi, Y. Tsujimoto, Y. F. Guo, S. B. Zhang, Y. Matsushita, M. Tanaka, Y. Katsuya, K. Kobayashi, K. Yamaura, and E. Takayama-Muromachi, Phys. Rev. B **83**, 100410(R) (2011).

[53] V. Hardy, C. Martin, G. Martinet, and G. André, Phys. Rev. B **74**, 064413 (2006).

[54] S. Ishiwata, D. Wang, T. Saito, and M. Takano, Chem. Mater. **17**, 2789 (2005).

[55] X. Yao, J. Phys. Chem. A **116**, 2278 (2012).

[56] M. Lenertz, J. Alaria, D. Stoeffler, S. Colis, and A. Dinia, J. Phys. Chem. C **115**, 17190 (2011).

[57] Z. He, J.-I. Yamaura, Y. Ueda, and W. Cheng, J. Am. Chem. Soc. **131**, 7554 (2009).

[58] W. Shiramura, K.-i. Takatsu, B. Kurniawan, H. Tanaka, H. Uekusa, Y. Ohashi, K. Takizawa, H. Mitamura, and T. Goto, J. Phys. Soc. Jpn. **67**, 1548 (1998).

[59] E. Lieb, T. Schultz, and D. Mattis, Ann. Phys. **16**, 407 (1961).

[60] D. C. Cabra, A. Honecker, and P. Pujol, Phys. Rev. B **58**, 6241 (1998).

[61] G. Giri, D. Dey, M. Kumar, S. Ramasesha, and Z. G. Soos, Phys. Rev. B **95**, 224408 (2017).

[62] S. Thomas, S. Ramasesha, K. Hallberg, and D. Garcia, Phys. Rev. B **86**, 180403(R) (2012).

[63] P. Y. Huang, C. S. Ruiz-Vargas, A. M. van der Zande, W. S. Whitney, M. P. Levendorf, J. W. Kevek, S. Garg, J. S. Alden, C. J. Hustedt, Y. Zhu, J. Park, and P. L. McEuen, Nature (London) **469**, 389 (2011).

[64] V. Kochat, C. S. Tiwary, T. Biswas, G. Ramalingam, K. Hsieh, K. Chattopadhyay, S. Raghavan, M. Jain, and A. Ghosh, Nano Lett. **16**, 562 (2016).

[65] K. Balasubramanian, T. Biswas, P. Ghosh, S. Suran, A. Mishra, R. Mishra, R. Sachan, M. Jain, M. Varma, R. Pratap, and S. Raghavan, Nat. Commun. **10**, 1090 (2019).

[66] R. Pariser and R. G. Parr, J. Chem. Phys. **21**, 466 (1953); J. A. Pople, Trans. Faraday Soc. **49**, 1375 (1953).

[67] S. R. White, Phys. Rev. Lett. **69**, 2863 (1992).

[68] S. R. White, Phys. Rev. B **48**, 10345 (1993).

[69] M. Kumar, Z. G. Soos, D. Sen, and S. Ramasesha, Phys. Rev. B **81**, 104406 (2010).

[70] J. C. Bonner and M. E. Fisher, Phys. Rev. **135**, A640 (1964).

[71] S. K. Saha, D. Dey, M. Kumar, and Z. G. Soos, Phys. Rev. B **99**, 195144 (2019).